

# Effects of Temperature conditions on the synthesis of nanocrystalline hydroxyapatite by using polyol method

Bochra Dhoub, Nourredine Jouini, Mongia Hosny, Valérie Bockelee, Frederic Schoenstein, Hafed EL Feki  
 Laboratoire des Sciences des Matériaux et Environnement, Faculté des sciences de Sfax, 3010 Sfax, Tunisie.

Laboratoire des Propriétés Mécaniques et Thermodynamiques des Matériaux, LPMTM, CNRS UPR 9001  
 Université Paris XIII, 99 Avenue J.B. Clément, 93430 Villetaneuse, France

**Abstract:**-Nanoparticles of hydroxyapatite (HA) were synthesized by involves precipitation and hydrolysis reactions conducted in polyol medium under atmospheric pressure. It was found that the solvent had an effect on the formation of HA and degree of crystallinity and temperature as well. The influence process of was discussed in details. The crystal morphology and particle size were analyzed by Transmission Electron Microscopy (TEM), the thermal analysis by TGA/DTA and the compositions and chemical structures were identified by X-ray diffraction (XRD) and Fourier Transform Infrared Spectroscopy (FTIR).

**Keywords:** hydroxyapatite, nanoparticle, polyol medium, temperature reaction.

## I. INTRODUCTION

Hydroxyapatite  $\text{Ca}_{10}(\text{PO}_4)_6(\text{OH})_2$  (HA) has great importance in chemistry materials because of its excellent biocompatibility [1]. In addition, it was shown that many clinical capabilities of HA depend mainly on morphology and HA particles size [2]. In recent years, significant research efforts have been devoted to developing the preparation and morphology control method of HA powders. Up to these days, the influence of the morphology of micro- and nanoparticles on their biodistribution has been mostly unknown. However, only a few studies have suggested that the shape of objects introduced in the body has a major influence on their fate in fluids [3], in vitro [4], and in vivo. Thus, the observation of micro-organisms shows that shape not only influences their displacement but also their capacity to interact with both the cells and the capture by macrophages. At the micro- and nanometric levels, the influence of shape on the interaction between particles and cells presents an undeniable scientific and pharmaceutical interest. HA powders with various morphologies were synthesized by means of solid-state reaction [5], sol-gel method [6], template-directed method [7] hydrothermal method [8]-[9], micro emulsion [10] emulsion technique [11] and precipitation from aqueous solutions accomplished in an organic solvent to the so-called polyol process or, more usually in water [12]. Accordingly, much attention has been paid to the polyol process study as it has several advantages. It is well known that the subtle microstructure of nanoparticles can be tailored by altering some major

synthesis parameters, such as reactant concentration, stirring, maturation, addition rate [13], temperature reaction and solvent [14]. Indeed, basing on many experimental data, the polyol process has an impact on the composition, the morphology, and the dimensions of the solids formed in the heterogeneous system. Note that alcohol itself acts as a stabilizer, limiting particle growth and prohibiting agglomeration. Our team's effort was focused on the preparation of HA nanoparticles using common chemical precipitation method and hydrolysis reactions conducted in polyol medium, investigating the solvent factor and finding the influence of parameter temperature related to the crystal nucleation and the growth/dissolution of phases HA. HA nanoparticles were synthesized and a series of process conditions, which were supposed to influence the nucleation, size and morphology of HA particles, were studied by means of single factor test method and the possible influence process was discussed.

## II. EXPERIMENTAL METHOD

### A. Parameters of synthesis

In order to obtain nanometric apatitic particles, we made use of the synthesis per wet process in polyol medium method. In fact, we used the ethylene glycol (EG) solvent. This process consists in pouring a solution containing the cations of  $\text{Ca}^{2+}$  (calcium nitrate) drop by drop on a solution containing anions  $\text{PO}_4^{3-}$  (diammonium phosphate  $(\text{NH}_4)_2\text{HPO}_4$ ), with Ca/P ratio 10:6, using a peristaltic pump during 3 h. To adjust the pH of the solution at 10, we added an ammonia solution. In order to investigate the relationship between crystalline growth and temperature, the procedure for fabricating hydroxyapatite was synthesized at various temperatures such as 100, 137 and 198 °C termed HA-100, HA-137 and HA-198, respectively. The solution was left for a one – hour maturation. A column with backward flow was also used to prevent the losses of liquid by vaporization. After cooling, the product was filtered and washed with ebullient water and ethanol then dried with the drying oven during 24 h.

### B. Characterization

The samples were analyzed by powder X-ray diffraction (Philips,  $\text{CuK}\alpha$ ). Besides, the structural information was obtained starting from a powder diagram

collected in the angular field 5–110 in 2 $\theta$  with an angular step of 0.04 (2 $\theta$ ) and counting time of 5 s. The XRD peak broadening enabled us to measure the crystallite size in a perpendicular direction to the crystallographic plane on the condition that the broadening arises entirely as a result of size effects. The crystallite size (D)(hkl) perpendicular to a crystallographic plane (hkl) could be evaluated by measuring the full width at half maximum (EWHM) according to the Scherrer formula:

$$(d)(hkl) = \frac{K\lambda}{B \cos \theta(hkl)} \quad (\text{Equation (1)}) [15]$$

Where (d) is the crystallite size (nm); K is the shape factor (K is 0.9 when the particles are spherical);  $\lambda$  is the wavelength of the X-rays ( $\lambda = 1.5406 \text{ \AA}$  for Cu K $\alpha$  radiation); B is the FWHM (rad) and  $\theta$ (hkl) is the Bragg's diffraction angle ( $^{\circ}$ ). With regard to the FT-IR spectra (JASCO 420) which were recorded in the range of 400–4000  $\text{cm}^{-1}$  using KBr pellet technique. The measurement of specific surface was conducted in the process of adsorption into multi-layer of nitrogen gas at a low temperature by means of an automatic sorpiometer (Quanta chrome Autosorb Al-C) and according to the theory of BRUNAUER, EMETT and TELLER (BET). The ground powders were also examined by thermo gravimetric analysis (SETARAM Instrumentation, thermal analysis, TG). Besides, the DTA analysis of the HA powders was performed in a Perkin- Elmer at a heating rate of 20  $^{\circ}\text{C}/\text{min}$ . The size and morphology of the particles as well as the microstructure of the consolidated samples were studied using a JEOL-2011 Transmission Electron Microscope (TEM) operating at 200 kV.

### III. RESULTS AND DISCUSSION

The reactions involved in the formation of HA during the polyol medium preparation and drying can be expressed as follows:

$10\text{Ca}(\text{NO}_3)_2 \cdot 4\text{H}_2\text{O} + 6\text{KH}_2\text{PO}_4 \longrightarrow 20\text{NH}_4\text{OH}$   
 $\text{Ca}_{10}(\text{PO}_4)_6(\text{OH})_2 + 6\text{KOH} + 20\text{NH}_4\text{NO}_3 + 52 \text{H}_2\text{O}$   
 (Equation (2)) The formation of 20NH $_4$ NO $_3$  (ammonium nitrate) by product was removed by repeated washing with double distilled water. Fig. 1 shows XRD patterns of HA products prepared at different reaction temperatures 100 $^{\circ}\text{C}$ , 137 $^{\circ}\text{C}$  and 198 $^{\circ}\text{C}$  designated as HA-100, HA-137 and HA-198 and a fixed pH value (10) with aging time (1 h). XRD patterns of HA-198 powders, which indicate the desired final product, show no presence of phases HA. Although, XRD diffraction patterns of HA-137 show some characteristic peaks of HA could be also observed at the angles of 26 $^{\circ}$  and 30–34 $^{\circ}$ , corresponding to the (002), (211), (112) and (300) diffractions. So it could be well indexed to the hexagonal Ca $_5$ (PO $_4$ ) $_3$ (OH) in P63/m space group (JCPDS No. 09-0432) and other crystalline phases calcium phosphate hydrate (Ca $_2$ (P $_2$ O $_7$ )(H $_2$ O) $_4$ , JCPDS N $^{\circ}$ .01-070-4788), Calcium Hydrogen Phosphate (Ca(H $_2$ PO $_4$ ) $_2$ , JCPDS N $^{\circ}$ .09-390)

and  $\beta$ -TCP(JCPDS N $^{\circ}$ .09-169) were present, implying the incomplete reaction between diammonium phosphate and calcium nitrate tetra hydrate. XRD diffraction patterns of HA-100 at 100 $^{\circ}\text{C}$  contained sharp peaks and exactly match of HA and no other crystalline phase was present. The spectra show that the aspect ratio, the stoichiometry and the thermal stability of obtained HA are all strongly dependent on the temperature of the hydrolysis. A critical evaluation of the literature revealing the precipitation reaction is usually conducted ranging from room temperature to temperatures close to (though not at) the boiling point of water [16]. The solubility behavior of hydroxyapatite is not only characterized by a persistent and high super saturation with respect to HA, but by HA dependence on the solution temperature. The temperature is characterized by a systematic dependence of the ion activity product of this compound on the mixture composition and the solubility product principle for HA. In this way, it is the surface layer which will ultimately control the solubility behavior of HA. This phenomenon suggests that certain reactions occur at the hydroxyapatite/ phase interface upon equilibration. These reactions may be limited to a preferential adsorption of calcium or phosphate ions or they may react with the surface layer of the HA particles. However, the latter may result in a diffusion barrier which finally prevents further dissolution of the crystals HA. From the dissolution data obtained under leaching conditions at 137 $^{\circ}\text{C}$  and 198 $^{\circ}\text{C}$ , we conclude that a surface complex was formed with the composition on the basis of similarities between the structure of HA and that of family calcium phosphates. Thus, the theoretical solubility behavior could be predicted from the extrapolated value $\bar{e}$  of the free energy for the found products [17] As seen in the XRD pattern, the peaks were broad, which brought to light the smaller size of the crystallite/particle in the powder. The diffraction peaks at 2 $\theta$  values corresponding to (211) and (300) Miller planes, were respectively selected for the calculation of the crystalline size using Equation (1). Furthermore, as seen in Fig 1, both peaks were relatively sharper than the other peaks. This corresponds to the crystal growth following the c-axis of the hexagonal HA structure, as reported in the literature. Using the formula (Equation (1)), the crystallite size (d) of the synthesized HA powder was calculated to be 17.3 nm in the case of EG for plane (211) and 13 nm in the case for plane (300).

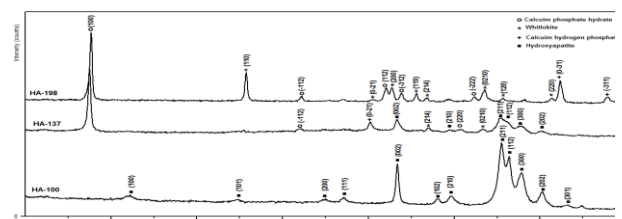


Fig. 1: XRD patterns of the preparation HA powders at different temperatures.

The thermo gravimetric analysis of the as-prepared HA-100 powders in the temperature range of 25–1200°C, is represented in Fig. 2(a). In fact, their curves show a four-stage weight loss at the temperature range of 25–200°C, 200–400°C, 400–750°C and 750–950°C. In the first stage, an obvious weight loss was observed indicating the evaporation of the adsorbed water from the surface and pores [18]-[19]. In the second stage, losses were due to the lattice water waste [20]-[21]. In the third stage, the loss can be attributed to B type carbonate decomposition [22]. In the final stage and at higher temperatures, carbonate decomposition takes place. The total weight loss is about 7.5% (EG). However, there was no further weight loss on heating up to 950°C, which indicated the high thermal stability of the samples. The DTA curves of the as-prepared HA powders, whose obtained results proved the existence of four endothermic peaks, is represented in Fig. 2 (b). In fact, while the first two peaks corresponded to the loss of residual water, the second and third endothermic peaks were attributed to the decarbonation (in both types). It proved that the majority of the recorded phenomena were similar to those observed for a hydroxyapatite prepared by wet process in aqueous medium.

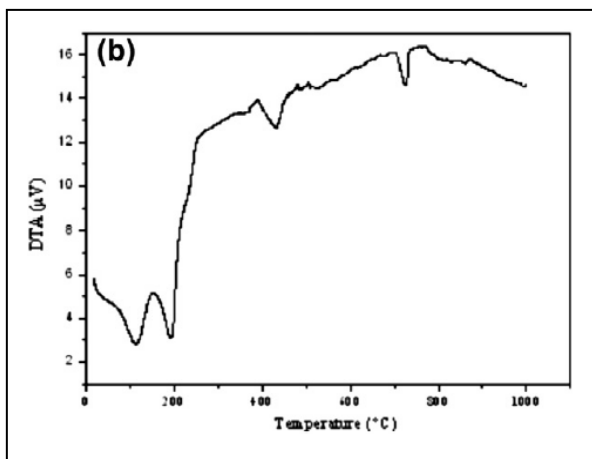
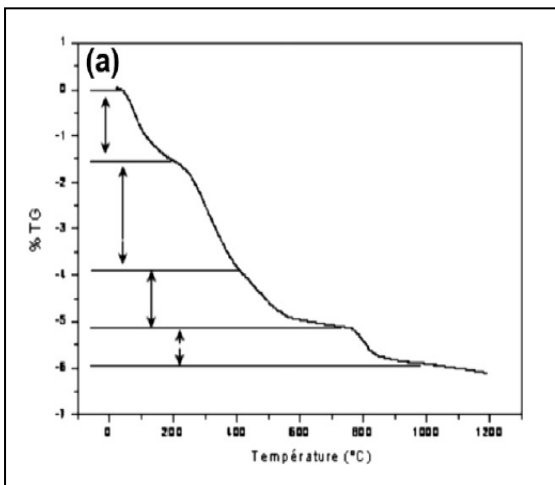


Fig. 2: (a) Curve TGA of the powder of HA-100 (b) Curve ATD of thermal decomposition of HA-100

Rietveld analysis (Fig.3) was performed for HA powder calcined at 950 °C (HA-950) because the decarbonation was confirmed by DTA showing a carbon dioxide evolution until 950°C. Pattern fitting was carried out between 10° and 90°. The lower bar shown in Fig 3 indicated the fitting deviation from the lower original diffraction pattern. An effective separation of these overlapping data was created by the “Rietveld Method” and hence allowed an accurate determination of the structure. As shown in Fig.3, the lower bar, which indicates a pure powder, is perfectly in harmony with XRD peaks. Lattice dimensions (*a*-, *b*- and *c*-axis dimensions) were calculated for the fitted peaks. They were determined as *a* = 0.9405 nm, *b* = 0.9405 nm and *c* = 0.687 nm with angles  $\alpha = \beta = 90^\circ$  and  $\gamma = 120^\circ$  indicating a hexagonal unit cell structure. These values were in close proximity with unit cell dimensions of HA crystals of tooth enamel reported previously in the literature [23].

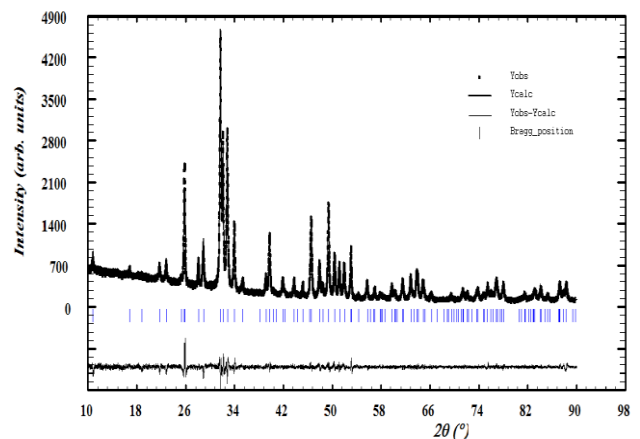


Fig. 3: Rietveld analysis of HA-950 powders.

FTIR patterns presented in Fig. 4 confirmed the formation of HA calcined at 950 °C (HA-950). The vibrational and stretching modes of OH- in the apatite lattice appeared at 631 cm<sup>-1</sup> and 3570 cm<sup>-1</sup>, respectively. In addition, a strong band of PO<sub>4</sub><sup>3-</sup> group was also seen at 1100, 1037 and 965 cm<sup>-1</sup> corresponded to P–O stretching vibration modes ( $\nu_3$  and  $\nu_1$ ), the doublet at 603-564cm<sup>-1</sup> and the band at 472 cm<sup>-1</sup> corresponded to O–P–O bending modes ( $\nu_4$  and  $\nu_2$ ).

The bands obtained for respective phosphate and hydroxyl groups of pure HA, were in agreement with other published data [24]. A weak band of CO<sub>3</sub><sup>2-</sup> was detected in the region around 1435 cm<sup>-1</sup>. This band indicates that a minor amount of carbonate substitution occurred [21]. The features bands of inorganic carbonate ion prove that carbon did not pyrolyze completely but got dissolved in the organics from atmosphere and thus might dissolve into the HA crystal. Because carbonates are constituents of bone structures [25] the presence of CO<sub>3</sub><sup>2-</sup> may play a vital role in the bioactivity of HA rather than being a cause of concern.

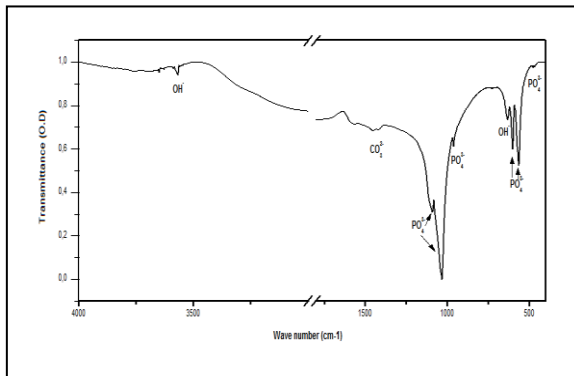


Fig. 4: FTIR of HA-950 powders.

Fig. 5(a) clearly shows the shape of the particles not calcined HA in EG. The incongruent nucleation and growth behavior of hydroxyapatite are made according to two different geometrical forms; the first is plates owing to two directions while the second is needles due to a privileged direction that is probably the C direction. This morphology of the particles could be attributed to the relative specific surface energies associated with the different planes of HA crystal or nucleus. These different planes having different surface energies are going to work out the quantity of OH<sup>-</sup> absorbance from the solution [26]. In our case, the different planes will have OH<sup>-</sup> concentration as the solution prepared is maintained at a high pH = 10, which will fix out the growth rate and morphology of the crystal. As for the particles which adopt the shape of plates, they admit a length varying from 140 to 200 nm and a width from 60 to 80 nm with almost constant thickness (15– 20 nm). Nevertheless, the dimensions of needles vary from 10 to 14 nm in diameter and from 100 to 200 nm in length. All the irregularities of surface existing on a molecular scale are taken into consideration by the specific surface. The specific surface of the powder of non-calcined HA is obviously high. It is resulted in according to B.E.T method, resulting in 87 m<sup>2</sup>/g for the particles corresponding to the HA. After calcining at 950°C and according to Fig. 5(b), the particles of HA assume a more increasing morphology.

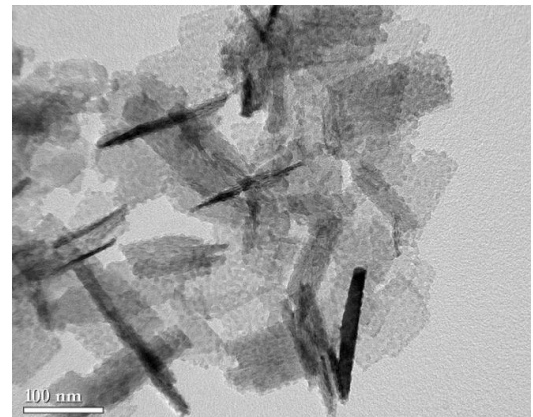
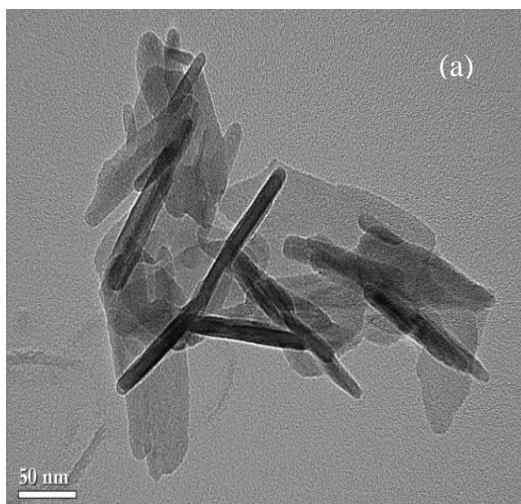


Fig.5: (a) TEM image of HA not calcinated (b) TEM image of calcinated HA at 950°C.

#### IV. CONCLUSION

HA powders were synthesized by double decomposition in polyol medium at different temperature. The results indicated that preparing temperature were critical in controlling synthesis of the HA particles. When the preparation temperature was at 100°C, XRD analysis of resulting products revealed a single crystalline phase, similar to stoichiometric HA. When the preparation temperature was higher, secondary phases were detected and the phase HA was present at 137°C but with an increase in the temperature, it was noticed a disappearance of HA. Thus, the initial Temperature value played an important role in the phase formation of HA, and initial temperature at 100°C was beneficial to the formation of pure HA. The analysis of HA proved that the materials obtained were of pure and stoichiometric apatite, which was well defined at calcining temperature 950°C. This simple synthesis method can be extended to prepare other interesting substituted hydroxyapatite nanomaterials.

#### REFERENCES

- [1] QJ. He, ZL. Huang, "Controlled growth and kinetics of porous hydroxyapatite spheres by a template-directed method," *Journal of Crystal Growth*, Vol. 300, pp. 460–466, March 2007.
- [2] JC. Elliot, "Recent studies of apatites and other calcium orthophosphates," in: E. Bres, P. Hardouin (Eds.), *Calcium phosphate materials, fundamentals*, Sauramps Medical, Montpellier, 1998.
- [3] F. Ye, HF. Guo, HJ. Zhang, XL. He, "Polymeric micelle-templated synthesis of hydroxyapatite hollow nanoparticles for a drug delivery system," *Acta Biomaterial*, Vol. 6, pp. 2212–2218, June 2010.
- [4] YC. Wang, AH. Yao, WH. Huang, DP. Wang, J. Zhou, "In situ fabrication of hollow hydroxyapatite microspheres by phosphate solution immersion," *Journal of Crystal Growth*, Vol. 327, pp. 245–250, July 2011.

- [5] S. Pramanik, AK. Agarwal, KN. Rai, A. Garg, "Development of high strength hydroxyapatite by solid-state-sintering process," *Ceramics International*, Vol. 33, pp. 419–426, April 2007.
- [6] G. Bezzi, G. Celotti, E. Landi, TMG. La Torretta, I. Sopyan, A. Tampieri, "A novel sol–gel technique for hydroxyapatite preparation," *Materials Chemistry and Physics*, Vol. 78, pp. 816–824, February 2003.
- [7] YJ. Wang, SH. Zhang, K. Wei, NR. Zhao, JD. Chen, XD. Wang, "Hydrothermal synthesis of hydroxyapatite nanopowders using cationic surfactant as a template", *Materials Letters*, Vol. 60, pp. 1484–1487, June 2006.
- [8] J. Liu, X. Ye, H. Wang, M. Zhu, B. Wang, H. Yan, "The influence of pH and temperature on the morphology of hydroxyapatite synthesized by hydrothermal method," *Ceramics International*, Vol. 121, pp. 59–64, 2002.
- [9] IS. Neira, YV. Kolenko, OI. Lebedev, GV. Tendeloo, HS. Gupta, F. Guitián, M. Yoshimura, "An effective morphology control of hydroxyapatite crystals via hydrothermal synthesis," *Crystal Growth Design*, Vol. 9, pp. 466–474, 2009.
- [10] YX. Sun, GS. Guo, DL. Tao, ZH. Wang, "Reverse micro emulsion-directed synthesis of hydroxyapatite nanoparticles under hydrothermal conditions," *Journal of Physics and Chemistry of Solids*, Vol. 68, pp. 373–377, March 2007.
- [11] GK. Lim, J. Wang, SC. Ng, LM. Gan, "Formation of nanocrystalline hydroxyapatite in nonionic surfactant emulsions," *Langmuir*, Vol. 15, pp. 7472–7477, 1999.
- [12] PP. Wang, CH. Li, HY. Gong, XR. Jiang, HQ. Wang, KX. Li, "Effects of synthesis conditions on the morphology of hydroxyapatite nanoparticles produced by wet chemical process," *Powder Technology*, Vol. 203, pp. 315–321, November 2010.
- [13] BL. Cushing, VL. Kolesnichenko, CJ. O'Connor, "Recent advances in the liquid-phase syntheses of inorganic nanoparticles", *Chemical Reviews*, Vol. 104, pp. 3893–3946, 2004.
- [14] A. Mechay, H. EL Feki, F. Schoenstein, N. Jouini, "Nanocrystalline hydroxyapatite ceramics prepared by hydrolysis in polyol medium," *Chemical Physics Letters*, Vol. 541, pp. 75–80, 2012.
- [15] LA. Azaroff, "Elements of X-ray crystallography," McGraw-Hill, New York. pp. 38–42, 1986.
- [16] M. Sadat-Shojai, MT. Khorasani, E. Dinpanah-Khoshdargi, A. Jamshidi, "Synthesis methods for nanosized hydroxyapatite with diverse structures," *Acta Biomaterial*, Vol. 9, pp. 7591–7621, August 2013.
- [17] FCM. Driessens and RMH. Verbeeck, "Metastable states in calcium phosphate - aqueous phase equilibrations," *Journal of Crystal Growth*, Vol. 53, pp. 55–62, May 1981.
- [18] H. Füredi-Milhofer, V. Hlady, FS. Baker, RA. Beebe, N. Wolejko-Wikholm, JS. Kittelberger, "Temperature-programmed dehydration of hydroxyapatite," *Journal of Colloid Interface Science*, Vol. 70, pp. 1–9, June 1979.
- [19] MA. Larmas, H. Hayrynen, LHJ. Lajunen, "Thermo gravimetric studies on sound and carious human enamel and dentin as well as hydroxyapatite," *Scandinavian Journal of Dental Research*, Vol. 101, pp. 185-191, August 1993.
- [20] M. Ashok, NM. Sundaram, SN. Kalkura, "Crystallization of hydroxyapatite at physiological temperature," *Materials Letters*, Vol. 57, pp. 2066-2070, April 2003.
- [21] JC. Elliot, "Structure and Chemistry of the Apatites and Other Calcium Orthophosphates," Elsevier, Amsterdam, April 1994.
- [22] H. EL FEKI, C. Rey & M. Vignoles, "Carbonate ions in apatites: Infrared investigations in the  $\nu_4$  CO<sub>3</sub> domain," *Calcified Tissue International*, Vol. 49, pp. 269-274, October 1991.
- [23] AEW. Miles, "Structural and chemical organization of teeth," Academic Press II, New York, 1967.
- [24] I. Rehman, W. Bonfield, "Characterization of hydroxyapatite and carbonated apatite by photo acoustic FTIR spectroscopy," *Journal of Materials Science: Materials in Medicine*, Vol. 8, pp. 1–4, 1997.
- [25] AH. Rajabi-Zamani, A. Behnamghader, A. Kazemzadeh, "Synthesis of nanocrystalline carbonated hydroxyapatite powder via nonalkoxide sol–gel method," *Materials Science and Engineering C*, Vol. 28, pp. 1326–1329, December 2008.
- [26] J. Liu, X. Ye, H. Wang, M. Zhu, B. Wang, H. Yan, "The influence of pH and temperature on the morphology of hydroxyapatite synthesized by hydrothermal method," *Ceramics International*, Vol. 29, pp. 629–633, 2003.

E-mail

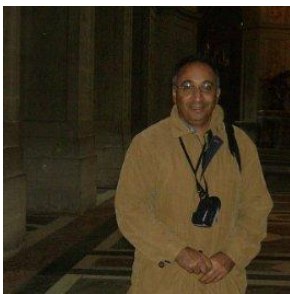
Hafed.

elfeki@yahoo.fr  
Tel : 216 74 276 400

Fax : 216 74 274 437

**AUTHOR BIOGRAPHY**

Nom et prénom : DHOUIB Bochra  
Date et lieu de naissance : 27/01/1986  
Dernier diplôme : Master de recherche  
Fonction : doctorante  
E-mail : [dhoubbochra86@yahoo.com](mailto:dhoubbochra86@yahoo.com)  
Tel : 21692020631



Nourredine Jouini,  
[nourredine.jouini@lspm.cnrs.fr](mailto:nourredine.jouini@lspm.cnrs.fr) 1984:  
Professeur des Universités à l'Université centrale de Tunisie  
1992-2002:

2003 : Maître de Conférences à  
l'université Paris Diderot (Paris 7)  
Professeur des Universités à l'université Paris 13Nord chercheur  
Laboratoire des sciences des Procédés et des Matériaux-LSPM-CNRS  
à diriger des recherches Chimie des matériaux- Nanomatériaux  
2010: Chef du département HSE, IUT de  
Saint-Denis, Université Paris 13  
2011: Membre du conseil d'administration à l'université Paris  
13Nord



Nom & Prénom	EL
FEKI Hafed	
Date et lieu de Naissance	12
Février 1961 Sfax Tunisie	
Dernier diplôme	Thèse
de Doctorat d'Etat Es-Sciences en Chimie	
Fonction	Profes
seur des Universités	
Laboratoire / Centre	Recherche
toire des Sciences des Matériaux et d'environnement, LR/ 05/ ES12	Labora
Adresse	Professionnelle
sité de Sfax, Faculté des Sciences de Sfax, Tunisie	Univer